

# East Greenland and the Faeroe Islands: A Fission Track Study

By SOHAN L. KOUL, LEWIS T. CHADDERTON,  
*and* C. KENT BROOKS

Det Kongelige Danske Videnskabernes Selskab  
Matematisk-fysiske Meddelelser **40**:13



Kommissionær: Munksgaard  
København 1983

## Synopsis

A study has been made of the etching characteristics of fission fragment tracks in certain zeolites, including chabazite, stilbite and heulandite, collected from the Upper, Middle and Lower Series basalt in the Faeroe Islands. Etching conditions with respect to annealing temperature have been standardized and optimized, with special attention being given to chabazite, and annealing experiments have been carried out on this mineral in order to derive the appropriate correction curve for application to igneous activity over geological time. It is shown that chabazite, employed as a solid state detector, registers fission fragment tracks anisotropically. Studies of the influence of both annealing the sample and varying the etchant temperature reveal no improvement in the degree of isotropy. Nevertheless the fission track method is applicable to the dating of chabazite in particular, and almost certainly for the dating of zeolites in general. Fission track dating of the Faeroe Islands yields a spread of corrected ages from  $41.6 \pm 1.1 \times 10^6$  y. to  $55.4 \pm 2.6 \times 10^6$  y., which are substantially less than ages obtained previously using radiometric methods.

Fission track ages are also reported for the minerals zircon, sphene and apatite, and for a few micaceous minerals – particularly phlogopite – collected from alkaline igneous intrusions in East Greenland (the Kangerdlugssuaq and Gardiner intrusions, and the island of Aliuarssik). The correction curve for phlogopite has been determined in laboratory annealing experiments. Extrapolation of the experimentally determined temperatures for annealing suggests that a temperature of 195°C will erase all tracks in  $\sim 10^6$  y. The annealing data is therefore interpreted in terms of the paleoisotherm of the fission track clock in the mineral.

The results obtained for the Faeroe Islands indicate a relatively short time span for the volcanic activity, a general conclusion which is not at variance with earlier radiometric studies, and which is consistent with the results for contemporaneous East Greenland lavas. The geological histories of the three selected areas of East Greenland, and differences between them, are discussed in the light of the fission track ages uncovered. For the Kangerdlugssuaq intrusion in particular it is proposed that there is clear evidence for strong doming and regional uplift, and that this was paralleled by a similar behaviour at the same time, although on a less grand scale, in an extensive area west of the Faeroe islands. The linkage in time of similar activity in the two geographical zones has implications in the dating of plate motions and for continental break-up of the North Atlantic province.

SOHAN L. KOUL

LEWIS T. CHADDERTON

Division of Chemical Physics, CSIRO,

P.O. Box 160, Clayton, Victoria, Australia 3168

C. KENT BROOKS

Institute of Petrology, University of Copenhagen,

Øster Voldgade 5, 1350 Copenhagen K, Denmark

(from 1. February 1983: University of Papua, New Guinea)

## List of Contents

I	Introduction .....	5
II	The Geology of the Faeroe Islands .....	6
III	The Geology of East Greenland .....	7
IV	The Etching Behaviour of Damage in Zeolites with Particular Reference to Chabazite as a Track Detector .....	8
V	The Annealing Correction to Fission Track (FT) Ages .....	15
VI	Fundamentals of Fission Track (FT) Dating .....	20
VII	Results .....	23
	VII.1. The Faeroe Islands .....	23
	VII.2. Greenland .....	24
	(i) The Kangerdlugssuaq Intrusion .....	28
	(ii) The Gardiner Intrusion .....	31
	(iii) Aliuarssik .....	32
VIII	Conclusion .....	33



## I. Introduction

The ways in which fission track (FT) procedures are normally applied in geology to determine times of mineral crystallization and ages of rock strata are now well understood. The general method itself has seen wide acceptance; there have been applications in such diverse disciplines as archaeology,<sup>1-3</sup> cosmology<sup>4-12</sup> and biology<sup>13-16</sup>. Since its introduction by FLEISCHER et al.<sup>17</sup> a growing number of laboratories have employed the FT technique in a variety of interdisciplinary studies.

This rapid growth in the importance of the FT technique is due in part to the maturity which certain of the experimental procedures have reached, not only in straightforward dating of igneous and metamorphic events,<sup>18-23</sup> but also in stratigraphic studies by the dating of ash layers,<sup>24,25</sup> the elucidation of rock uplift history,<sup>26-28</sup> and in the measurement of uranium, thorium and plutonium concentrations in various materials of both terrestrial and extraterrestrial origin. There have also been surprising applications in such unexpected fields as paleozoology<sup>29</sup> and botany.<sup>30,31</sup> Moreover, there are hopes that FT methods may hold the key to a solution of some of the most urgent problems confronting geochronology and cosmochronology today.

In this paper we describe in particular reconnaissance studies of the fission track dating of zeolites, a complex group of tectosilicates which is, for example, widely developed in basaltic rocks subsequent to their emplacement by later stage processes. Zeolites have assumed increasing importance in recent years due to a rapidly expanding interest in hydrothermal systems and in detailed studies of oceanic floors, as a consequence of the demonstration that typical volcanic areas have been permeated by huge quantities of hot water of meteoric origin,<sup>32</sup> and because of the need to understand hydrothermal processes in connection with the exploration and utilization of geothermal energy. The chemical etching conditions have been standardized by investigations of the temperature dependence of the etching behaviour for certain zeolites (in particular the minerals chabazite, stilbite and heulandite) and, for chabazite, have been used to study the track recording and retention characteristics in some detail, with particular reference to fossil hydrothermal systems in the Faeroe Islands. In order to check the general reliability of the method on zeolites, samples from the Faeroe Islands were selected in such a way that for some of them comparison could be made with age estimates established on geological grounds. Further experiments have been made to determine the calibration curve relating track length shrinkage with track density reduction – an important element in all fission track geochronology

Fission track ages are also reported for minerals in alkaline igneous rocks from the Tertiary deposits of East Greenland, since this zone has held a key position during formation of the North Atlantic, and since both volcanic and epeirogenic events are better displayed here than in any other geographic area around that sea.

## II. The Geology of the Faeroe Islands

The Faeroe Islands lie at the extreme northwestern edge of the European continental margin which consists here of a series of banks extending from the Rockall Plateau northwards to the Faeroe Plateau, a distance of about 1000 km. These banks are separated from the European Shelf by the Rockall trough and The Faeroe-Shetland Channel, a deep water area of partially unknown structure. The banks themselves are underlain with continental material and are therefore believed to be microcontinents detached from the European shelf by ocean-floor spreading. Indeed, inclusion of the Rockall and Faeroe Plateaus in pre-drift reconstructions<sup>33</sup> considerably improves the fit of continental models from which they have been omitted.<sup>34</sup>

The Faeroe Islands themselves cover about 1,400 km<sup>2</sup> and are the erosional remnants of a Lower Tertiary basaltic plateau which may once have been as extensive as 24,000 km<sup>2</sup>, the area of the insular shelf. The basalts are similar in structure, composition and age to those of East Greenland and have an exposed thickness of about 3,500 m, although the top and bottom of the sequence are not seen. Our knowledge of the geology of the islands stems mainly from the work of RASMUSSEN and NOENYGAARD,<sup>35,36</sup> and from that of WAAGSTEIN,<sup>37</sup> who also studied the insular shelf and the neighbouring banks. The exposed sequence is divided into three series; the Lower, Middle and Upper Basalts. The Lower Basalts (Fig. II.1), consist almost exclusively of aphyric and slightly plagioclase-phyric, olivine-poor, lava flows with a thickness averaging about 20 m. They are separated from the Middle Basalts by a distinctive horizon of volcanogenic sediments and coal, while the Middle Basalts begin explosively with the deposition of up to about 100 m of pyroclastics (a tuff-agglomerate zone). Typical Middle Basalts differ from the Lower Basalts in being thin pahoehoe units averaging about 2 m in thickness. Most are plagioclase-phyric, but olivine-phyric and aphyric flows, and a single orthopyroxene-phyric flow, also occur. The base of the Upper Basalts (Fig. II.2) is marked by a prominent group of olivine-phyric and aphyric flows which have been shown to form very flat shield volcanoes of great areal extent. The Upper Basalts are a comparatively variable group but are typically characterized by olivine-phyric, LIL-element depleted flows which are best developed in the northeastern and northern parts of the islands. There is still evidence for unconformities in the Faeroe lava sequence and it is believed that jointing, faulting and gentle warping are subsequent to the extensive phase. Many dikes and sills cut the lavas and these intrusives also seem largely to postdate major Basaltic flows.



Fig. II.1. The western side of Kunoy seen from Kalsoy in The Faeroe Islands. The lavas have a very shallow dip and the base of the Upper Basalts is at the first thick horizon going up to the top. Mountains are up to about 800 m (A. Noe-Nygaard).

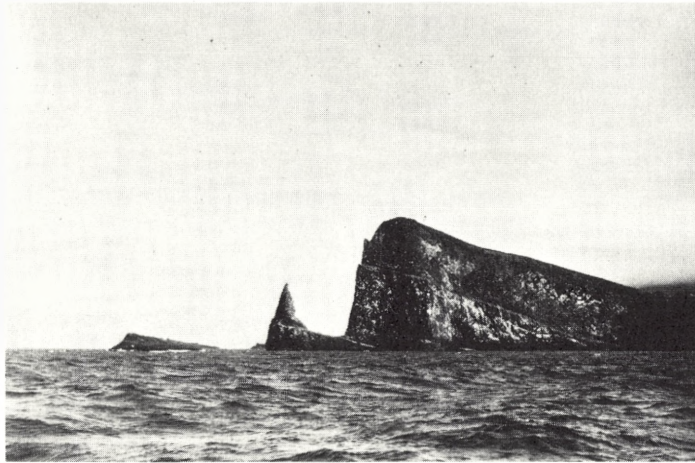


Fig. II.2. Lower Basalts on Mykinesholmur in the Faeroe Islands showing a relatively steep easterly dip. The cliff is just over 100 m (A. Noe-Nygaard).

### III. The Geology of East Greenland

The Tertiary rocks of the east of Greenland (Fig. III.1) originally covered an area of some 100,000–200,000 km<sup>2</sup>. They were deposited in the Lower Tertiary in connection with continental break-up in the North Atlantic and, as such, are part of the North Atlantic igneous province whose continuing activity still is evident in Iceland. Rock types in East Greenland include volcanics which are largely voluminous plateau basalts of tholeiitic composition, and a wide spectrum of intrusives, including layered

gabbros (e.g., the famous Skaergaard intrusion), granites, syenites and nepheline syenites (e.g., the Kangerdlugssuaq intrusion) with minor amounts of others. Recent reviews of the province have been published by one of us,<sup>38</sup> and by other workers.<sup>39-41</sup>

Briefly, the evolution of the province was as follows. After a long period continental conditions emerged, and subsidence with accompanying sedimentation began towards the end of the Cretaceous in the Kangerdlugssuaq area. In more northerly areas continental rifting had been active throughout most of the Mesozoic. Outpouring of basaltic lavas, mostly of tholeiitic character but some picritic, subsequently commenced and filled up the basin rapidly so that, although the first lavas are submarine, the bulk of the plateau is subaerial. There is, however, evidence that subsidence still continued but not at a rate rapid enough to keep pace with the volcanic accumulation. The total thickness of basaltic products is thought to have locally attained some 7 km.<sup>42</sup> The basalts themselves were erupted via a fissure swarm parallel to the present coast line, where dike swarms occur which are sometimes so intense as to make up 100% of the total outcrop. Associated with this extensive activity the newly forming continental margin became attenuated and flexured in the direction of the embryonic ocean floor. Numerous gabbroic bodies were emplaced in and close to the dike zone. Radiometric dating results allied with biostratigraphic evidence<sup>43,44</sup> indicate that these events took place around the Palaeocene-Eocene boundary (53-54 m.y ago).

While the magmatic activity along the coast was almost exclusively tholeiitic, areas inland experienced minor alkaline activity characterized by nephelinites similar to those of the African continent. After a few million years of relative quiescence syenitic bodies were largely emplaced in the Kangerdlugssuaq area. Brooks<sup>45</sup> has suggested that this phase here was accompanied by a major crustal doming event (fig. III.2) which he delineated. At the present erosional level, syenites and related rocks are the most voluminous Tertiary bodies exposed and, apart from minor dike swarms, represent the final stages of local magmatism. Conversely, in the Kialineq (67°N) area, a number of felsic plutons were emplaced at about 35 m.y.<sup>60-62</sup> and, to the north, the Werner Bjerge pluton (72°N) was active at around 30 m.y.<sup>46-49</sup>

#### IV. The Etching Behaviour of Damage in Zeolites with Particular Reference to Chabazite as a Track Detector

The fact that solid state track detectors (SSTD's) can tolerate large neutron doses without detectable deterioration makes them uniquely suitable for measuring the concentrations of certain heavy elements in specific samples. Presently glasses, plastics and a limited number of single crystalline materials are being used in applications of FT methods,<sup>50-52</sup> and in addition there is ample evidence that SSTD's are not only the





Fig. III.1. East Greenland basalts inland from the northern part of the Blosseville Kyst. They remain relatively undisturbed and have only been subjected to regional uplift. Tops of the mountains in this area are very close to the original top of the basalt pile (Geodetic Institute, Copenhagen).



Fig. III.2. Inner part of the Kangerdlugssuaq-Nordfjord (Greenland) extending into the left, with the Kangerdlugssuaq Gletscher Snout at the bottom. The plateau to the distant left is an exhumed Pre-Tertiary peneplain which was covered by basalts. To the right is the Kangerdlugssuaq dome carved in uplifted Precambrian gneisses.

best integrating type of detector for swift heavy charged particles, but can be used for fast neutron detection.<sup>53-56</sup> Studies are also being made of the effects of high fast neutron doses on track registration generally and on the thermal stability of tracks. Crystalline detectors have been used less frequently than glasses and plastics in part, at least, because they are more temperature-resistant. Moreover, the bulk etch rate velocity  $V_g$  examined by various investigators in crystalline detectors such as bronzite,<sup>57</sup> feldspar,<sup>58,59</sup> sphene,<sup>60</sup> and labradorite,<sup>57</sup> has been shown to be anisotropic.

Experiments were first carried out to determine the effect of etching at various temperatures, the effect of heat on the anisotropic properties of chabazite used as a track detector, and a systematic search made for a suitable etchant to reveal tracks in the zeolites chabazite, stilbite and heulandite. Track recording and retention characteristics for chabazite, however, will be described in detail. The FT etching efficiency of a mineral is defined as that fraction of the total number of fission fragments to have crossed a given surface which is visible in the optical microscope. If the rate of chemical etching is very much greater than the general rate of etch, then due to the fact that the etchant penetrates along the full length of the damage trajectory, the majority of tracks are revealed as hollow cylinders, and the efficiency is high, as is the case with chabazite.

Our investigations have concentrated upon the suitability of the solvents NaOH and KOH for chabazites in particular. Homogeneous, inclusion-free chabazite crystals from Vágur were selected for this study. Samples were prepared by first using normal grinding methods to the finer stage, and then polishing with diamond abrasives ranging from the 8  $\mu$  to the 0.5  $\mu$  grades, after which the samples were divided into two groups. To determine the appropriate etchant for chabazite, samples from the first group were etched in boiling NaOH for times varying from a few minutes to several hours, the density of spontaneous tracks due to natural fission being measured at discrete intervals. We found neither the track geometry nor the variation of track density with time to be satisfactory. After trying a number of other solvents, a satisfactory etching of the chabazite specimens was finally accomplished using KOH (3g in 4g H<sub>2</sub>O). Again the samples were etched for from a few minutes to several hours and the track density measured after each time step. It is a clear characteristic of KOH that, compared with NaOH, this etchant gives an almost uniform distribution of tracks, with better defined contours. The results (Figure IV.1) indicate that with NaOH a maximum in track density is reached, followed by a slow decrease due to progressive chemical removal of surface layers of the crystal. For KOH, a plateau, which is reached rather quickly, remains invariant with time (Figure IV.2).

The second group of samples was annealed for 2 hour at 540°C (further details are given in section V) in order to erase all spontaneous tracks. Artificial tracks were then created using a <sup>252</sup>Cf source in a 2 $\pi$  geometry and chemical etching experiments carried out on two sets for different times, using NaOH and KOH. Again, in the case of KOH, a constant track density plateau was reached after a short time (Figure IV.2). These different relationships for various etchants are due to fundamental differences in the velocity of etching along the tracks ( $V_r$ ) relative to that for the bulk solid ( $V_g$ ). The ratio  $V_r/V_g$  is high for KOH in the case of chabazite. It is much lower for NaOH.

A few samples of chabazite were annealed at 540°C for two hours, mounted in epoxy resin along the cleavage plane, and mechanically polished in order to investigate both possible effects of track orientation and of heating on the registration efficiency of

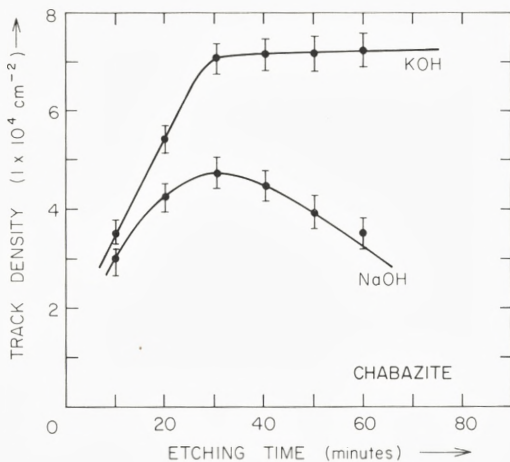


Fig. IV.1. Etching rates of chabazite for NaOH and KOH (spontaneous fission tracks).

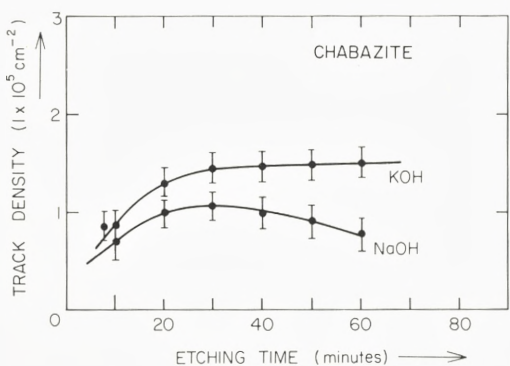


Fig. IV.2. Etching rates of chabazite for NaOH and for KOH (induced (artificial) fission tracks).

chabazite. The polished samples were irradiated from a  $^{252}\text{Cf}$  source in a  $2\pi$  geometry for equal times in order to implant the same number of fission fragments. The angular track distribution was then obtained by measuring the inclination of the ends of tracks relative to a fixed, but arbitrary direction, the analysis being carried out using both optical and scanning (SEM) microscopes. The distribution of etched tracks in the  $\{10\bar{1}1\}$  plane for different etching times is shown in Figure IV.3. It is quite clear that, beyond a certain minimum etching time, the track density remains constant. Similar results have been reported by NISHIDA and TAKSHIMA<sup>61</sup> and KOUL et al.<sup>62</sup> However, it may be shown that for certain materials the track density or an internal surface continues to increase with prolonged etching. With glass, for example, there is a further exposure of new tracks as the surface is progressively attacked by the etchant. These are then added to the previous tracks which remain visible with continued

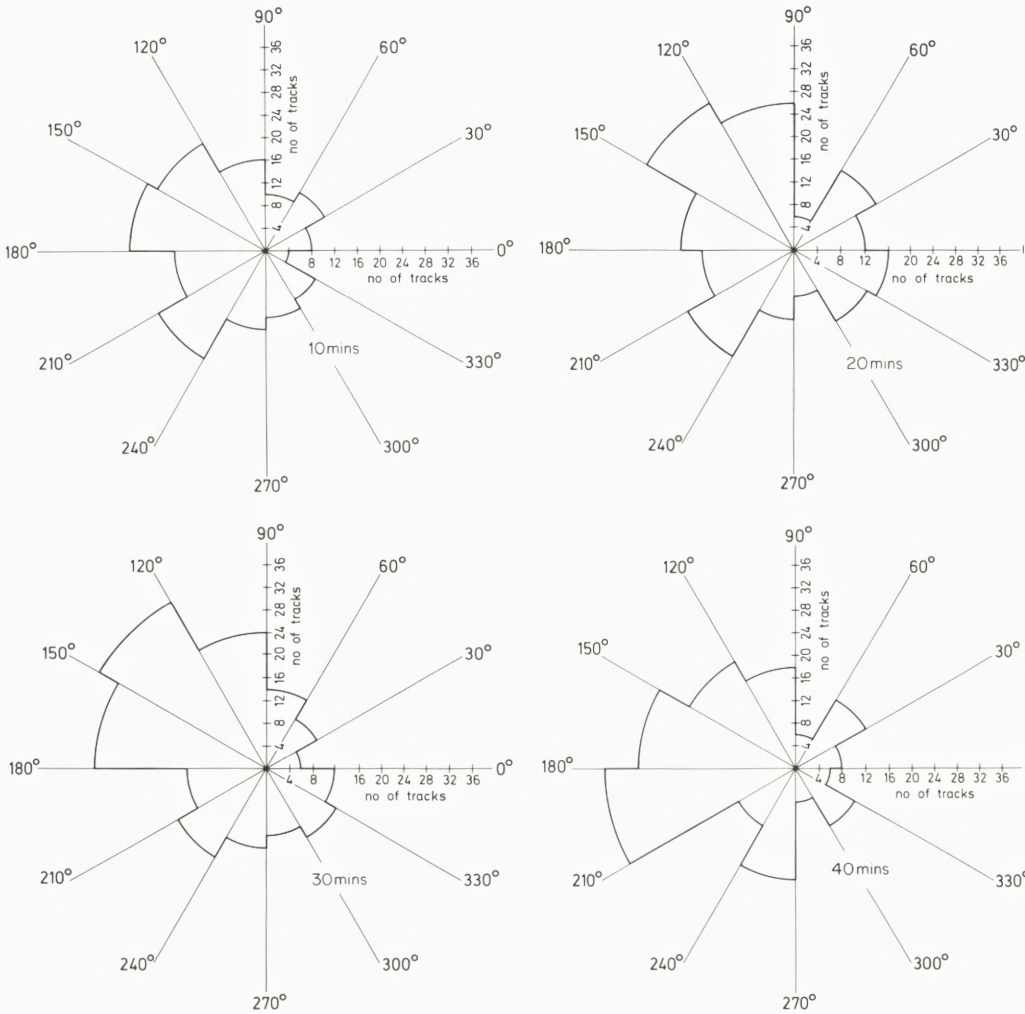


Fig. IV.3. Sets of contour lines showing the angular distributions of etched tracks in the  $\{10\bar{1}1\}$  plane obtained by etching the same chabazite sample for 10, 20, 30 and 40 minutes in KOH. The efficiency and the degree of isotropy with increasing etching are not improved.

etching. In the case of chabazite etched in KOH this effect does not occur. The present experiment demonstrates in addition that the etching of  $\{10\bar{1}1\}$  chabazite at different temperatures, however prolonged, does not improve the degree of isotropy of the etched tracks. Other crystal planes ( $\{1\bar{1}01\}$  and  $\{01\bar{1}2\}$ ) gave identical results.

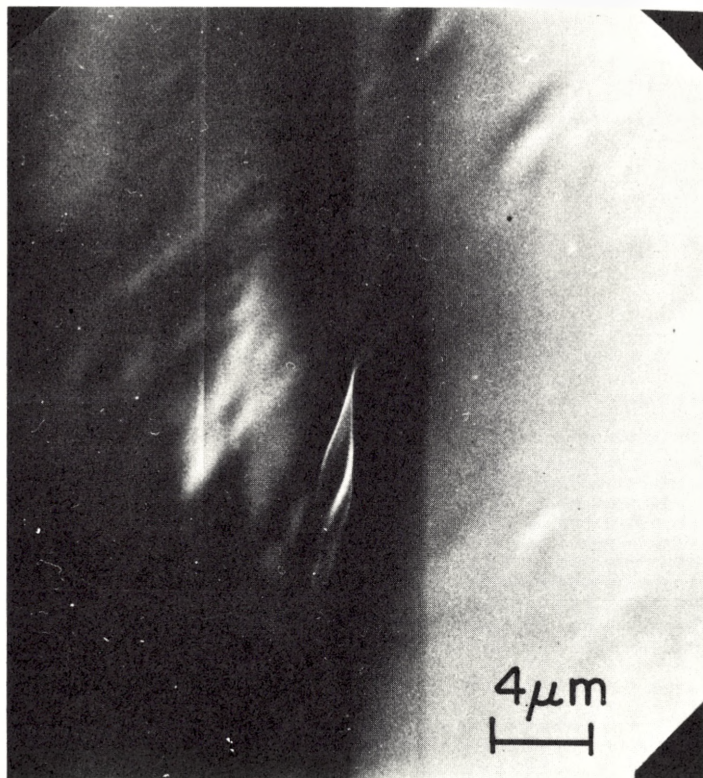
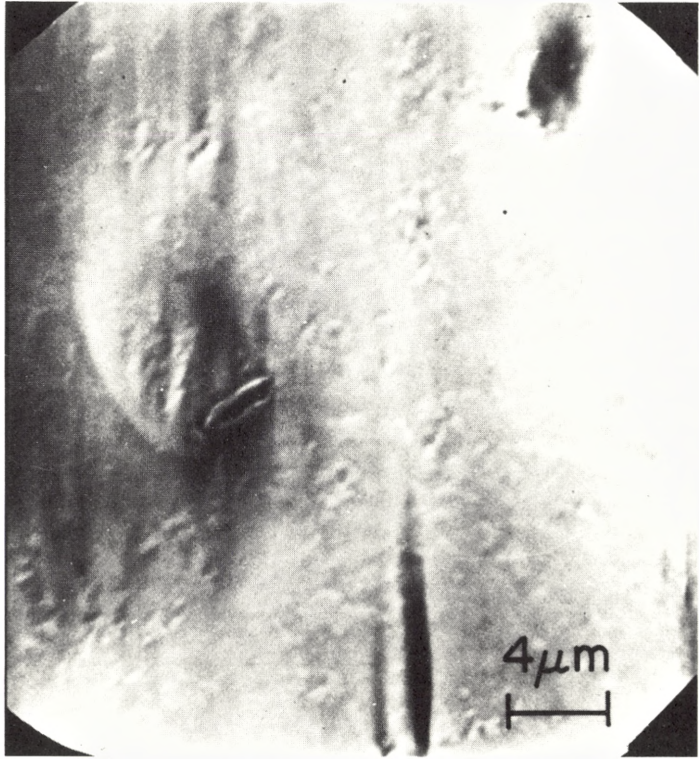


Fig. IV.4. Scanning electron micrograph of a fission fragment track in chabazite, etched in KOH (3 g in 4 g H<sub>2</sub>O). The micrograph was taken at a dip angle of 45°.

Experiments were also carried out to determine the *relative* effect of heating on the degree of isotropy of the etched tracks in the  $\{10\bar{1}1\}$ ,  $\{\bar{1}101\}$  and  $\{01\bar{1}2\}$  planes. Samples of chabazite were heated at different temperatures and afterwards etched in KOH for the appropriate length of time. No amount of prior annealing improved the isotropy of the tracks in a sample. We conclude that the anisotropic etching behaviour of fission fragment damage trails is accordingly a natural and inherent property, unaffected either by etching or heating.

The brief scanning electron microscope (SEM) study of fission fragment damaged chabazite was made in order to examine etched tracks at a higher magnification. Samples of chabazite of about 1–2 cm<sup>2</sup> in area were irradiated in the thermal column of the reactor to a total thermal neutron dose of 10<sup>15</sup> nvt in order to induce fission of uranium impurity atoms. These samples were then polished down to a thickness of ~ 3 microns, and etched in the appropriate chemical reagent (see earlier sections) for the appropriate length of time. After evaporation of a thin layer of gold the samples were examined in the JEOL instrument. Figure IV.4 shows a single fission track in a

Fig. IV.5. Scanning electron micrograph of a fission fragment track in chabazite, etched in KOH (3 g in 4 g H<sub>2</sub>O) after heating at 400°C for 1 hour. No substantial change is observed although the track is reduced in size due to annealing.



chabazite specimen tilted to an angle of 45°. Annealing was carried out at successively higher temperatures (ranging from 100–500°) in an attempt to observe any change with temperature in the morphology of a typical etched fission track. No substantial change was observed in the 100–300°C temperature range, though at 400°C tracks were reduced in size due to annealing (Figure IV.5). From the present study we therefore conclude that the shape of the etch pits does not change in different planes of the crystal when using the same chemical reagent, and there is no temperature dependence in the degree of track anisotropy in chabazite. The shape of the etch pits was different when the samples were etched in different chemical reagents. Different etchants, however, gave no improvement in the degree of anisotropy of chabazite when used as a track detector. The general etching velocity,  $V_g$ , apparently does not vary from plane to plane in the same crystal. It is more than likely that the anisotropy has its origin in the spatial variation of electronic stopping power  $Se$  for natural fission fragments moving in chabazite.<sup>63</sup>

## V. The Annealing Correction to Fission Track (FT) Ages

Due to the effect of thermal (igneous) annealing over geological time the ages of minerals determined by the fission track technique have on occasion been observed to be lower<sup>64-66</sup> than corresponding ages determined by the far more conventional radiometric methods.<sup>67,68</sup> No theory exists which can completely explain the annealing of radiation damage and rejuvenation of minerals on heating, though models have been proposed on the basis of limited experimental observations.<sup>69</sup> It is rather clear, however, that when a mineral is heated at high enough temperatures there is a return of some atoms to lattice sites and, although dislocations and other extended defects are formed, most of the strain present due to radiation damage disappears. The degree of the annealing in general depends both upon the temperature and the time of heating. For each mineral, however, there is a characteristic 'annealing temperature' at which measurable strain is totally removed; virtually complete restoration can be considered to have taken place.

Some possibility of the annealing of radiation damage and therefore of track fading in minerals always exists. The track fading can be caused by a short time, higher temperature event or by a lengthy anneal at only a slightly elevated temperature during the geothermal history of the earth's crust. The importance of thermal excursions which take place during the geological history of a sample and of the consequent effect upon the final fission track age must not be minimized. Experiments were accordingly carried out both to determine the extent of this effect and to provide a calibration curve for making the appropriate correction.\*

The specific mineral samples selected for this work included chabazite from Vágur (Faeroe Islands), and phlogopite from Gardiner, East Greenland. Both minerals were separated from crushed rock using common laboratory techniques, and samples polished by the usual procedures. After annealing chabazite at 520°C for 3 hours,\*\* and phlogopite at 570° for 3 hours, induced fission tracks were created at a thermal neutron dose of  $10^{15}$  (nvt). The fission fragment track density was then determined by etching aliquots, which had undergone heat treatments varying from 100 to 500° ( $\pm 5^\circ\text{C}$ ) for a period of one hour in each case, and the reduction of track density and track length was observed. A procedure for etching through different planes was adopted for the revealing of full length tracks. Length measurement itself was per-

\* STROZER and WAGNER<sup>70</sup> first proposed an appropriate method for correction of a thermally lowered track density, using calibration curves of residual track density as a function of average length of etch pit, both quantities being expressed as fractions of their unannealed values. The method has frequently been used in the correction of thermally lowered fission track ages;<sup>12,66,70-74</sup> it is applicable both to glasses<sup>12,73</sup> and minerals.<sup>66,75-78</sup>

\*\* It is important to note that the chabazite crystal structure only begins to break down at approximately 840°C.<sup>79</sup>

formed by measuring both track dip and projected length, and optical phase contrast methods used to enhance precision. An average of 'major' and 'minor' axes for each etch pit was recorded as the corresponding 'etch pit length'. For almost 9000–11000 etch pits scanned a total of between 800 and 900 track lengths were measured – an extremely lengthy and laborious process but one absolutely necessary for proper statistics. Figure V.1 shows how the reduction in track density and track length in chabazite depends upon temperature. This kind of information makes possible an immediate estimate of the degree of fading of the spontaneous tracks, and hence the reduction in age. At 100°C, a slight decrease of ~ 2.0% in track density and ~ 3.5% in the mean track length of etch pits was observed in the case of chabazite. At higher temperatures, the track length decreased more rapidly than the track density. At a constant temperature of 500°C a period of 1 hour reduced the track density by 57.3% and the track length by 78.3%. Following 1 hour at 600°C all tracks were completely annealed. In the case of phlogopite, changes in track length and track density at 100°C were almost negligible. At 100°C, a decrease of 3.5% in track length and *no* change in track density was observed. At higher temperatures, however, the track length decreased more rapidly than the track density as was precisely the case for chabazite. At 700°C, the track density was reduced by 60% and the track length by 69%. At 800°C all the tracks were annealed out, due to a phase change in the solid.

The observation that the reduction in track density with temperature lags behind the track length (Figure V.1) is important. Measurement of  $^{235}\text{U}$  induced fission fragment tracks in unannealed samples, and in samples which had been subjected to various annealing treatments, were therefore carried out. It is the shrinkage in track length, plotted as a function of track density reduction, which gives the proper calibration relationship. The ratio of mean etch pit length of unannealed and annealed fission tracks is shown as a function of the percentage of fission track density reduction in Figure V.2. The resulting calibration curve has been used to correct thermally lowered fission track ages of chabazite, and we find the correction to fission track ages to be ~ 3% for chabazite, and ~ 6% for phlogopite.

The stability of fission tracks varies from substance to substance. Indeed it is this very variation which gives rise to optimism as to the reconstruction of rock cooling histories, provided that the temperatures or temperature ranges below which the tracks are retained can correctly be estimated. Therefore, in some cases it is possible to learn about the igneous (annealing) activity which the mineral has endured over geological time. For example, in the case of phlogopite from the Gardiner complex of East Greenland, annealing studies confirm that fossil fission fragment tracks (radiation damage) in the mineral can be erased during intense metamorphic episodes, thus resetting the geological clock.

The fission track method has, of course, already proved to be a valuable technique for the dating of the mica group.<sup>27, 80–83</sup> Furthermore, the fact that these minerals have the



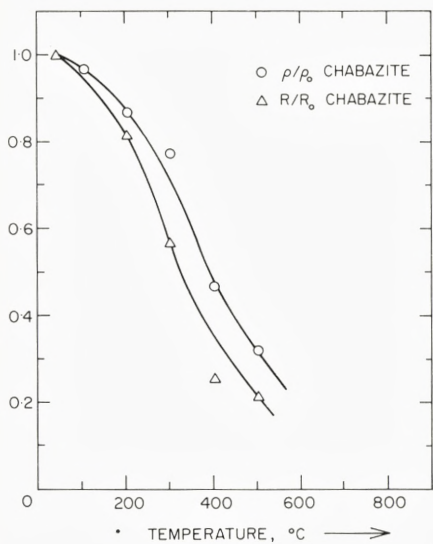


Fig. V.1. Normalized track densities  $\rho/\rho_0(0)$  and track lengths  $R/R_0(\Delta)$  displayed as a function of annealing temperature  $T$  for chabazite.

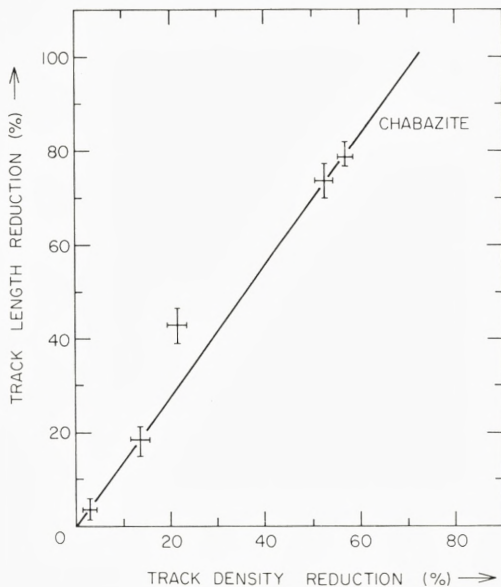


Fig. V.2. Percentage reduction of fission track lengths in chabazite shown as a function of the percentage reduction in fission track density.

potential for an unravelling of the geothermal history of the area of origin is well documented.<sup>20, 21, 84-86</sup> In what now follows we are primarily concerned with the thermal annealing behaviour of phlogopite in particular. The annealing data obtained is interpreted in terms of a palaeoisotherm of the fission track clock in the mineral. Measurement are also presented of the etchable "ranges" of spontaneous and induced fission tracks in the phlogopite samples.

In general the method most commonly used to study the annealing behaviour of minerals involves attention to the following:

- (1) The selected sample should have a uniform and large induced track density. It should be irradiated to a suitable thermal neutron dose in the reactor.
- (2) The sample should have a well defined and well polished plane and as uniform a distribution of uranium as possible.

After preparation of good phlogopite samples according to these criteria etching was accomplished by immersing the specimens in 40% HF at 23°C. The tracks, randomly distributed, could easily be distinguished from surface dislocations. Following deter-

mination of the *spontaneous* track density, samples were heated in a furnace in air (for 3 hours at 600°C) to anneal all fossil tracks, and then irradiated to a thermal neutron dose of  $10^{15}$  nvt in the thermal column of the reactor. They were then scanned in the optical microscope and the density of *induced* tracks was determined at a total magnification of  $\times 600$  using a  $5 \times 5$  ocular graticule. Studies were also made of the variation of track density as a function of temperature and time. The irradiated samples were recleaved in order to remove upper layers and any possible uranium contaminant of non-crystalline origin. These cleaved samples were then heated in a furnace at temperatures between 500°C at intervals of 30°C, and for times varying from a few minutes to several hours. They were then etched and scanned for any change of track density. The annealing data for phlogopite, shown in Figure V.3 represent 0%, 25%, 50%, 75%, and 100% track reductions, determined at various temperatures and corresponding to different times. The data have been extrapolated to geologically meaningful times and temperatures.

Annealing of fission tracks<sup>87</sup> has been reported for tektites,<sup>12, 88-90</sup> for epidote,<sup>91, 92</sup> for micas,<sup>66, 93</sup> for zircons<sup>94</sup> and for apatite. As Table 1 shows, each mineral has different annealing characteristics, and fission tracks in phlogopite anneal out at lower temperatures than those in muscovite and zircon. In almost every instance, however, the annealing rate is represented by a simple Arrhenius relationship:

$$\log_e t = \log_e a + \left( \frac{\epsilon}{kT} \right), \quad (1)$$

where  $t$  and  $T$  are the annealing time and temperature respectively,  $\epsilon$  is the activation energy,  $a$  is a material specific constant dependent on the degree of annealing, and  $k$  is Boltzmann's constant. Figure V.3 shows that phlogopite is no exception.

Phlogopite loses some fission tracks at  $\sim 45^\circ\text{C}$  in  $10^6$  years, and all tracks are erased at  $195^\circ\text{C}$  in  $10^6$  years.\*\*\*

From Figure V.3 it is also possible to make some assessment of the thermal history of a typical phlogopite of this type. Thus, if the fission track (FT) age agrees with an absolute age or ages determined by some other method, then the rock temperature must have remained to the right of the 0% track loss curve throughout. Conversely, if the FT age is less than those recorded by other methods, then the FT age implies that a geological cooling period has taken place. A "mixed" FT age results if the rock has been heated to such a temperature and for such a length of time that the corresponding point falls in the field between the 0% and 100% reduction in track density curves. Our

\*\*\* It has also been found that heating under pressure shows no detectable effect on the annealing properties of phlogopite. The annealing characteristics of zircon, on the other hand, are slightly affected by a hydrostatic pressure.<sup>94</sup>

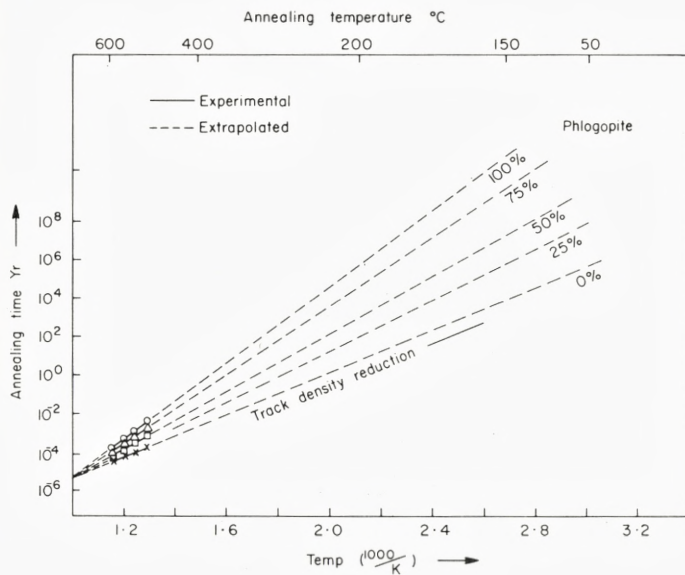
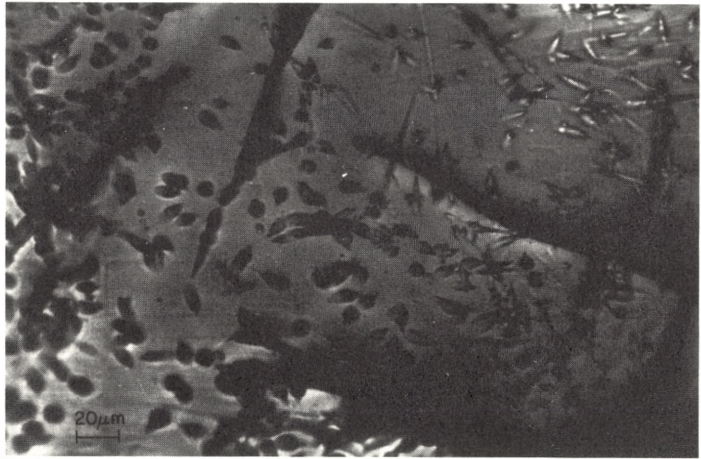
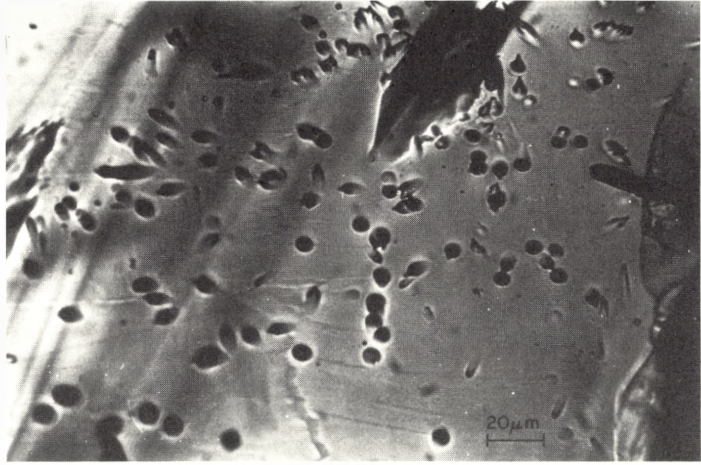


Fig. V.3. Annealing time as a function of annealing temperature for track density reductions in phlogopite of between 0% and 100%. Experimental results (—) are extrapolated to geologically meaningful times and temperatures (-----).

annealing experiments with phlogopite both confirm that fossil fission tracks are unstable and that the degree of instability varies from mineral to mineral. Furthermore, as with other radiometric methods, the FT age of phlogopite determines neither the age of mineralization nor the deposition age of the rock. It is the cooling age of the mineral which is established.

The demonstrable value of the fission track method has also stimulated specific laboratory experiments by a number of investigators on the track retention properties of minerals and glasses. The annealing data for certain minerals have been interpreted in terms of what might be called a "blocking temperature", which is a sharp transition of the palaeoisotherm at some time during the process of cooling. Different materials of course display different track retention properties, and the retention temperature depends upon the etching parameters, chemical variations in the material composition and on the track orientation.<sup>95</sup> All these factors have to be considered when annealing experiments directed at determining the thermal history of a sample (and its blocking temperature) are carried out. According to Haack<sup>96</sup> when a rock cools steadily to lower temperatures, the growth of track density increases linearly with time. For a specific cooling rate it is therefore possible to extrapolate back to a palaeotime of  $\sim 10^5$  to  $\sim 10^8$  years and hence to the temperature at which the track density was zero. Fission track blocking temperatures of various micaceous and accessory minerals, and some selected zeolites are compiled in Table VI.1. Temperatures are given both for full and half track fading, and for different annealing times.

Fig. VI.1. Photomicrographs showing spontaneous fission tracks in chabazite etched in KOH (3 g in 4 g H<sub>2</sub>O) (a), and induced fission tracks in chabazite irradiated with  $1.42 \times 10^{15}$  nvt thermal neutrons, and etched similarly (b).



## VI. Fundamentals of Fission Track (FT) Dating

The experimental FT technique used was similar to that of both NAESER and co-workers,<sup>91</sup> and KOUL and VIRK,<sup>20</sup> though with minor modifications which are briefly described. Thin transparent specimen sections approximately 0.5 mm across were separated from the host rock and mounted in epoxy resin, the upper surface of each sample being ground successively with 400, 600 and 800 mesh emery, polished with cerium oxide, and then followed by a final polishing with 6, 3, 1 and  $\frac{1}{4}$   $\mu\text{m}$  diamond paste. Samples of chabazite, stilbite, heulandite, apatite, sphene and zircon were

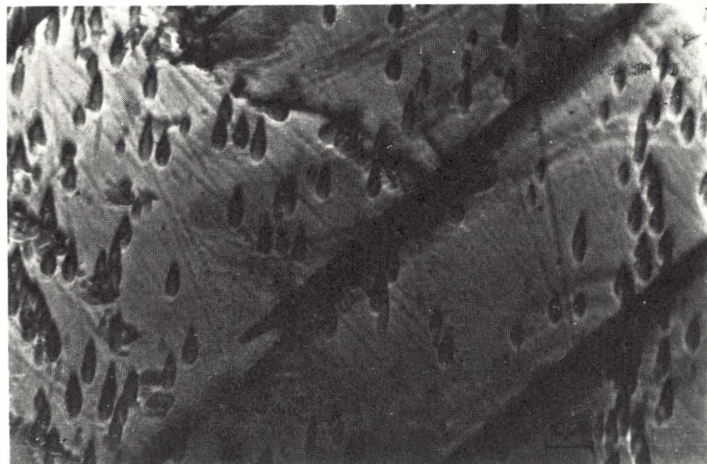


Fig. VI.2. Photomicrographs showing spontaneous fission tracks in stilbite etched in 2% HF at 23°C (a), and induced fission tracks in stilbite irradiated with  $7.12 \times 10^{15}$  nvt thermal neutrons, and etched similarly (typical anisotropic behaviour) (b).



treated identically, although the preliminary grinding was somewhat longer for crystals of zircon and sphene. Etching of the polished samples was by simple immersion in the appropriate chemical solvent.

The zeolites (chabazite, stilbite and heulandite) and the accessory minerals from igneous rocks (zircon, apatite and sphene) were all dated using the EDM (external detector) method;<sup>61,97</sup> samples were sandwiched between muscovite mica detectors for the registration and counting of induced tracks. Chabazite itself was etched in KOH (3 g in 4 g H<sub>2</sub>O) (see, e.g., Figure VI.1), while studies of various etchants for stilbite resulted in the use of 2% HF at 23°C for 20–30 secs (Figure VI.2), and 10 ml aqua regia

*Table VI.1*  
*Fission track retention and blocking temperatures of minerals*

Material	Degree of Loss	Annealing Temperature 1 hour °C	Blocking Temperature °C	Reference
Apatite	Half	336	108	(26)
	full	370	165	(21)
	full	400	170	(23)
	half	—	130	(110)
Australite	full	520	250	(111)
Biotite	full	500	—	(66)
	half	—	100	(110)
Basaltic glass	full	230	—	(112)
Chabazite	full	510	149	(62, 109)
Epidote	full	620	390	(113)
Garnet	full	545	—	(93)
	full	610	—	(109)
	full	545	—	(109)
Heulandite	full	495	—	(12)
Moldavite	full	495	—	(12)
Muscovite	full	700	—	(66)
Phlogopite	full	625	195	Present work
Stilbite	full	495	—	(109)
Sphene	half	610	350	(21)
Zircon	full	750	—	(23)
	full	870	—	(61)
	—	—	380	(114)

with 1 ml 2% HF at 23°C for 30–50 secs for heulandite. Zircon and sphene were etched in KOH: NaOH (the eutectic contains 50.6 mol % KOH and 49.4 mol % NaOH) at 200° for 8–20 hours and 50N.NaOH at 140° for 1–6 hours respectively. Apatite was etched in 5% HNO<sub>3</sub> for 20–30 secs, and phlogopite in 48% HF.

After determinations of spontaneous track density samples of all minerals were sandwiched between mica detectors and irradiated in the thermal column of the nuclear reactor. The integrated thermal neutron dose to which the samples were exposed was itself determined by counting tracks in a muscovite detector irradiated in contact with the standard NBS glasses SRM-962 and SRM-963 (calibrated against copper). The muscovite dosimeters were etched with freshly prepared 48% HF for 40–50 minutes at 23°C in order to obtain well defined induced tracks, approximately 800–1000 pits again being scanned for each consignment. An investigation of the general relationship between track counting on internal mineral surfaces and that on external

detectors was also made in order to determine the geometric factor for use of external detectors with zeolites. For the zeolites studied the geometric factor varied between  $0.51 \pm 0.02$  and  $0.57 \pm 0.03$ , assuming the etching rate and the counting efficiency for external detectors to be the same for each zeolite, and the track shape also to be the same. The track etching rate was always found to be greater than the general etching rate of the mineral surface. However, etching of tracks lying in different orientations was highly anisotropic giving rise to etch pits of varying topographic appearance. The constants used in the age calculations were  $\lambda_r$  (spontaneous decay of  $^{238}\text{U}$ ) =  $6.8 \times 10^{-17} \text{ yr}^{-1}$ ,  $\lambda_d$  (total decay constant of uranium) =  $1.551 \times 10^{-10} \text{ yr}^{-1}$ ,  $I$  (isotopic abundance of  $^{235}\text{U}$  with respect to  $^{238}\text{U}$ ) =  $7.253 \times 10^{-3}$ , and  $\sigma_f$  (cross-section for thermal neutron induced fission of  $^{235}\text{U}$ ) =  $5.802 \times 10^{-22} \text{ cm}^2$ . Errors were calculated throughout according to the methods of McGEE and JOHNSON<sup>98</sup> and NAESER et al.<sup>99</sup>, and expressed as one standard deviation.

## VII. Results

### VII.1. The Faeroe Islands

Our knowledge of the geology of the Faeroe Islands (section II and Figure VII.1) described by RASMUSSEN and NOE-NYGAARD<sup>100</sup> and WAAGSTEIN<sup>37</sup> may be considered to have been supplemented by SCHRØDER<sup>101</sup> who, on the basis of a limited magnetic survey, was able to demonstrate the presence of two domes centred to the west of the Islands. One of these lies just off Mykines where, on the most westerly point of the Islands (Mykines Holmur) the lavas attain an eastward dip of up to  $15^\circ$ . The other is to the southwest of Suduroy where a similar increase in dip occurs. This doming apparently affected the plateau subsequent to the volcanic activity, but may have overlapped and given rise to the tensional stress field which determined the emplacement of many of the minor intrusions.

WAAGSTEIN<sup>37</sup> reports the recovery of abundant reworked pyroclastic material from the sedimentary basins adjacent to the Islands, suggesting that the latest volcanic activity was submarine and due to submergence of the plateau. Thus volcanism and subsidence apparently kept approximate pace with each other as in the case of East Greenland. Uplift of the entire area took place later and the present mountain tops roughly define a gipfelflur ranging from about 800 m in the north to around half this in the central islands, and rising again to around 500 m on Suduroy. It is of considerable interest to determine the mechanisms of these vertical movements. The subsidence, doming and regional uplift strongly resemble those of East Greenland (although on a less grand scale). To this end it is important to establish the timing of these events.

It is clear from the field relationships that significant time gaps separated the three series, though this has not shown up in radiometric dating, from which variable ages

lying between  $49.2 \pm 1.5 \times 10^6$  up to  $60.4 \pm 1.4 \times 10^6$  y have been obtained.<sup>102</sup> Indeed, subsequent refinement of the data<sup>103</sup> suggests that the entire Faeroese lava pile from the bottom of the Lower to the top of the Middle Series was erupted in the interval  $55.2 \times 1.0 = 10^6$  y and  $54.6 \pm 1.2 \times 10^6$  y ago. Fission track results for chabazite, stilbite and heulandite shown in Table VII.1, for samples taken as shown in Figure VII.1, yield a spread of FT ages from  $41.6 \pm 1.1 \times 10^6$  y up to  $55.4 \pm 2.5 \times 10^6$  y, and the distribution of ages is such that the oldest value is from the Lower Series. However, we have no other evidence to contradict the general K-Ar results which indicate a relatively short time span for the volcanic activity, consistent with results from contemporaneous East Greenland and Faeroese lavas.<sup>104</sup> Our interpretation of the observed distribution is that it is most reasonably explained as being regional, the youngest ages in the north-eastern part of the Islands reflecting a more prolonged cooling there. This conclusion clearly requires an investigation of many more samples. It is consistent, however, with the belief of WAAGSTEIN<sup>37</sup> that volcanic activity had continued much longer than may be seen today, with the formation of overlying tuffs, since stripped away and deposited as clastic sediments on the insular shelf. If this activity had been confined to the north-eastern part of the islands, it would have provided an insulating cover which could have allowed hydrothermal circulation (with associated zeolite depositions) over a long period. Ages from the Lower Series on Suduroy and Mykines which are close to the accepted age of volcanism indicate that in the south and west of the islands the lavas underwent rapid cooling either as a result of lack of burial by significant amounts of overlying material, or as a result of very rapid uplift. Such a rapid uplift is likely to be a consequence of the dome-shaped structures believed to be present offshore to the north-west of Mykines and under Suduroy.<sup>100</sup> These domes, although on much smaller scale, invite comparison with East Greenland where a large domal uplift described by one of us<sup>45</sup> was raised shortly after the basaltic volcanism and rapidly dissected by erosion.



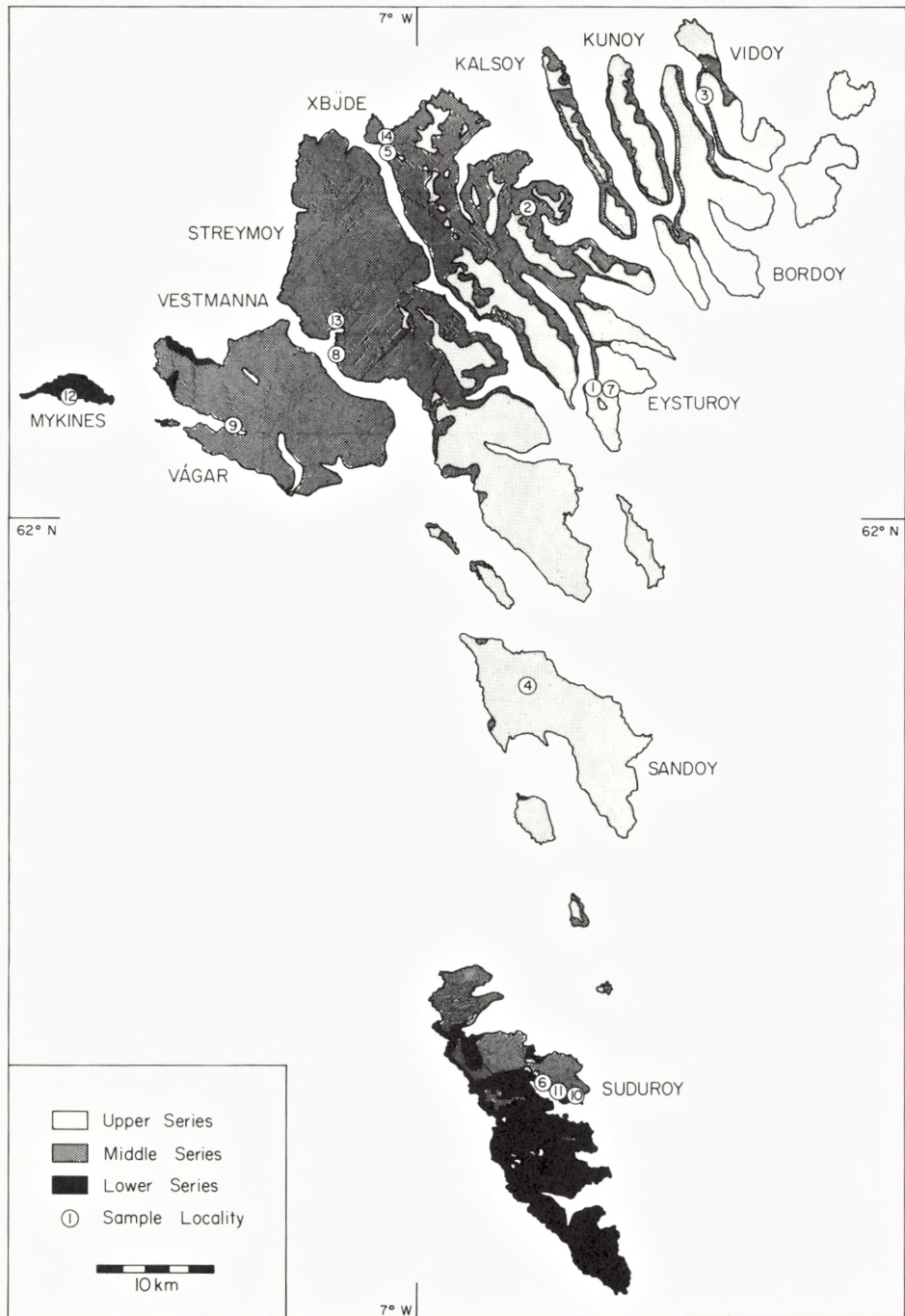


Fig. VII.1. Geological map of the Faeroe Islands (see reference 113).

*Table VII.1*  
*Fission track results for minerals from the Faeroe Islands*

Sample location*	Lab. symbols	$q_s$ ( $\text{cm}^{-2}$ )	$q_i$ ( $\text{cm}^{-2}$ )	$\Phi$ (nvt)	R	N	F.T. age (m.y.)
1. Chabazite. Runvik, Eysturoy. (U.S.)	CR105	$1.54 \times 10^4$	$1.73 \times 10^5$	$7.52 \times 10^{15}$	0.98	5	$41.2 \pm 1.8$
	CR109	$1.75 \times 10^4$	$1.73 \times 10^5$	—	0.965	5	$41.0 \pm 1.6$
	CR115	$1.68 \times 10^4$	$1.74 \times 10^5$	—	0.882	6	$44.7 \pm 2.0$
	CR116	$1.35 \times 10^4$	$1.48 \times 10^5$	—	0.865	8	$42.3 \pm 2.0$
	CR118	$1.92 \times 10^4$	$2.06 \times 10^5$	—	0.786	6	$43.2 \pm 2.1$
	CR120	$1.39 \times 10^4$	$1.41 \times 10^5$	—	0.744	7	$45.7 \pm 2.1$
	CR125	$1.42 \times 10^4$	$1.65 \times 10^5$	—	0.971	10	$40.0 \pm 1.8$
2. Chabazite. Slaettafjall, Eysturoy. U.S.	79-500/A1	$1.64 \times 10^4$	$3.50 \times 10^4$	$1.51 \times 10^{15}$	0.974	6	$43.5 \pm 1.6$
	79-500/A2	$1.82 \times 10^4$	$3.81 \times 10^4$	—	0.945	6	$44.4 \pm 1.6$
	79-500/A5	$1.35 \times 10^4$	$2.74 \times 10^4$	—	0.895	9	$45.7 \pm 2.0$
	79-500/A6	$1.95 \times 10^4$	$4.54 \times 10^4$	—	0.893	5	$39.9 \pm 1.9$
	79-500/A7	$1.74 \times 10^4$	$3.31 \times 10^4$	—	0.873	5	$48.8 \pm 2.1$
3. Chabazite. Malinsfjall, Vidoy. (U.S.)	79-2/C2	$1.48 \times 10^3$	$2.34 \times 10^4$	$9.80 \times 10^{15}$	0.745	6	$38.2 \pm 1.7$
	79-2/C5	$1.65 \times 10^3$	$2.41 \times 10^4$	—	0.894	8	$41.3 \pm 2.0$
	79-2/C6	$1.54 \times 10^3$	$2.23 \times 10^4$	—	0.981	6	$41.7 \pm 1.9$
	79-2/C8	$1.37 \times 10^3$	$1.95 \times 10^4$	—	0.984	4	$42.4 \pm 2.1$
	79-2/C9	$1.52 \times 10^3$	$2.20 \times 10^4$	—	0.989	7	$41.7 \pm 1.8$
4. Chabazite. Nordara, Sandoy. (U.S.)	79-95/A	$1.54 \times 10^4$	$3.52 \times 10^4$	$1.51 \times 10^{15}$	0.996	7	$40.7 \pm 1.7$
	79-95/7A	$1.73 \times 10^4$	$4.12 \times 10^4$	—	0.832	6	$39.1 \pm 1.9$
	79-95/8A	$1.64 \times 10^4$	$3.54 \times 10^4$	—	0.919	8	$43.1 \pm 2.0$
	79-95/11A	$1.94 \times 10^4$	$4.15 \times 10^4$	—	0.895	7	$43.3 \pm 2.1$
	79-95/1B	$2.34 \times 10^4$	$4.81 \times 10^4$	—	0.983	6	$45.2 \pm 1.9$
	79-95/5B	$1.34 \times 10^4$	$2.63 \times 10^4$	—	0.865	8	$47.3 \pm 2.2$
5. Chabazite. Eidi, Eysturoy, (M.S.)	CHVF1	$7.85 \times 10^4$	$1.42 \times 10^5$	$1.42 \times 10^{15}$	0.853	13	$48.3 \pm 1.1$
	CHVF2	$7.22 \times 10^4$	$1.34 \times 10^5$	—	0.764	8	$47.1 \pm 1.8$
	CHVF3	$6.84 \times 10^4$	$1.21 \times 10^5$	—	0.985	9	$49.4 \pm 1.6$
	CHVF5	$6.42 \times 10^4$	$1.15 \times 10^5$	—	0.982	9	$48.8 \pm 1.9$
	CHVF5	$7.35 \times 10^4$	$1.36 \times 10^5$	—	0.891	7	$47.3 \pm 1.9$
6. Chabazite. Suduroy, Tvöroyri. (L.S.)	CH205	$6.42 \times 10^4$	$3.22 \times 10^5$	$4.23 \times 10^{15}$	0.891	5	$51.9 \pm 3.1$
	CH207	$6.13 \times 10^4$	$3.12 \times 10^5$	—	0.980	8	$51.2 \pm 3.0$
	CH208	$5.84 \times 10^4$	$2.85 \times 10^5$	—	0.912	11	$53.4 \pm 3.1$
	CH231	$5.73 \times 10^4$	$2.91 \times 10^5$	—	0.943	7	$51.3 \pm 3.0$
	CH232	$6.02 \times 10^4$	$3.0 \times 10^5$	—	0.650	9	$52.3 \pm 3.2$
	CH239	$6.35 \times 10^4$	$3.21 \times 10^5$	—	0.960	5	$51.5 \pm 3.0$
7. Stilbite. Runavik, Eysturoy, (U.S.)	SRF1	$6.5 \times 10^4$	$1.38 \times 10^5$	$1.51 \times 10^{15}$	0.934	7	$43.8 \pm 1.2$
	SRF2	$7.2 \times 10^4$	$1.41 \times 10^5$	—	0.782	7	$47.5 \pm 1.8$
	SRF3	$6.3 \times 10^4$	$1.35 \times 10^5$	—	0.835	6	$43.4 \pm 2.0$
	SRF4	$4.5 \times 10^4$	$0.85 \times 10^5$	—	0.992	10	$49.2 \pm 2.1$
	SRF5	$7.2 \times 10^4$	$1.4 \times 10^5$	—	0.982	7	$47.8 \pm 1.9$

8. Stilbite.	43865/B	$1.34 \times 10^4$	$4.51 \times 10^4$	$2.48 \times 10^{15}$	0.984	8	$45.4 \pm 1.9$
Gassá-Breidá,	43865/B5	$1.47 \times 10^4$	$4.23 \times 10^4$	–	0.987	6	$53.1 \pm 2.3$
Stremoy	43865/B6	$1.68 \times 10^4$	$5.65 \times 10^4$	–	0.973	10	$45.4 \pm 1.9$
(U.S.)	43865/B7	$2.13 \times 10^4$	$7.54 \times 10^4$	–	0.931	9	$43.2 \pm 1.9$
	43865/BB	$1.54 \times 10^4$	$5.23 \times 10^4$	–	0.843	5	$45.1 \pm 2.0$
9. Stilbite.**	SK737	$3.25 \times 10^4$	$2.71 \times 10^5$	$6.24 \times 10^{15}$	0.862	5	$46.1 \pm 2.0$
Sörvágur,	SK835	$3.02 \times 10^4$	$2.7 \times 10^5$	–	0.938	4	$43.0 \pm 1.9$
Vágar.	SK1071	$2.72 \times 10^4$	$2.34 \times 10^5$	–	0.895	9	$44.7 \pm 2.0$
(M.S.)	SK1072	$2.85 \times 10^4$	$2.5 \times 10^5$	–	0.795	9	$43.8 \pm 2.1$
	SK1079	$3.12 \times 10^4$	$2.35 \times 10^5$	–	0.692	8	$51.0 \pm 2.2$
	SK1080	$2.24 \times 10^4$	$1.95 \times 10^5$	–	0.935	10	$44.2 \pm 2.1$
	SK1081	$2.90 \times 10^4$	$2.52 \times 10^5$	–	0.892	7	$44.2 \pm 2.0$
10. Stilbite.	18304/X3	$4.35 \times 10^4$	$1.26 \times 10^5$	$2.49 \times 10^{15}$	0.943	8	$52.9 \pm 2.8$
Hamar, Suduroy.	18304/X5	$5.24 \times 10^4$	$1.57 \times 10^5$	–	0.912	8	$51.2 \pm 3.0$
(L.S.)	18304/X6	$4.14 \times 10^4$	$1.21 \times 10^5$	–	0.981	7	$52.5 \pm 2.9$
	18304/X9	$3.27 \times 10^4$	$0.90 \times 10^5$	–	0.894	6	$55.7 \pm 3.2$
	18304/X10	$3.84 \times 10^4$	$1.14 \times 10^5$	–	0.895	5	$50.9 \pm 3.0$
	18304/X10A	$4.44 \times 10^4$	$1.32 \times 10^5$	–	0.794	5	$50.9 \pm 3.1$
11. Stilbite.	18301/FS	$4.32 \times 10^5$	$7.63 \times 10^5$	$1.51 \times 10^{15}$	0.878	5	$52.6 \pm 3.2$
Frodböur Kirke,	18301/FS2	$4.14 \times 10^5$	$7.25 \times 10^5$	–	0.985	10	$53.1 \pm 2.8$
Suduroy.	18301/FS7	$7.25 \times 10^4$	$1.23 \times 10^5$	–	0.913	6	$54.8 \pm 3.2$
(L.S.)	18301/FS9	$3.75 \times 10^5$	$7.13 \times 10^5$	–	0.986	7	$48.9 \pm 2.6$
	18301/FS10	$5.64 \times 10^5$	$9.87 \times 10^5$	–	0.895	6	$53.1 \pm 3.0$
	18301/FS13	$4.56 \times 10^5$	$7.65 \times 10^5$	–	0.764	5	$56.5 \pm 3.1$
12. Heulandite.	HL1	$4.72 \times 10^4$	$4.50 \times 10^5$	$8.04 \times 10^{15}$	0.970	5	$51.9 \pm 2.9$
Smörbúshelligjógv,	HL2	$5.12 \times 10^4$	$4.62 \times 10^5$	–	0.890	4	$54.8 \pm 3.1$
Mykines.	HL3	$4.81 \times 10^4$	$4.55 \times 10^5$	–	0.981	7	$52.3 \pm 3.0$
(L.S.)	HL5	$5.24 \times 10^4$	$4.64 \times 10^5$	–	0.973	8	$55.9 \pm 2.9$
	HL9	$4.65 \times 10^4$	$4.30 \times 10^5$	–	0.952	5	$53.5 \pm 3.0$
	HL10	$5.23 \times 10^4$	$4.75 \times 10^5$	–	0.895	6	$54.5 \pm 2.9$
	HL13	$4.90 \times 10^4$	$4.62 \times 10^5$	–	0.965	6	$52.5 \pm 2.8$
	HL8	$5.04 \times 10^4$	$4.21 \times 10^5$	–	0.891	8	$59.2 \pm 3.1$
13. Heulandite,	HG22	$3.45 \times 10^4$	$5.55 \times 10^5$	$9.64 \times 10^{15}$	0.772	6	$36.9 \pm 1.9$
Gassá-Breidá.	HG25	$4.51 \times 10^4$	$6.03 \times 10^5$	–	0.894	7	$43.7 \pm 1.8$
Vestmanna	HG28	$2.2 \times 10^4$	$3.04 \times 10^5$	–	0.983	8	$43.4 \pm 1.8$
Stremoy. (U.S.)	HG33	$5.34 \times 10^4$	$7.76 \times 10^5$	–	0.712	6	$40.9 \pm 1.9$
14. Heulandite,	HIE50	$8.04 \times 10^4$	$5.67 \times 10^5$	$5.64 \times 10^{15}$	0.882	5	$49.2 \pm 2.0$
Eidi, Eystoroy.	HIE55	$7.23 \times 10^4$	$5.24 \times 10^5$	–	0.813	5	$47.9 \pm 2.0$
(M.S.)	HIE57	$4.73 \times 10^4$	$3.65 \times 10^5$	–	0.954	9	$45.0 \pm 1.9$

$Q_s$  is the spontaneous track density,  $Q_i$  the induced track density,  $n$  the thermal neutron dose (nvt),  $N$  the number of grains counted, and  $R$  the correlation coefficient.

\* US, Upper Series; MS, Middle Series; LS, Lower Series.

\*\* Fissure-filling, all others are from amygdales.

## VII.2. Greenland

The East Greenland sector of the North Atlantic province is an exceptionally well exposed and well developed example of continental break-up which has been subject to a number of expeditions from Copenhagen with the specific object of documenting the magmatic and tectonic activity associated with this important phase of plate motions. In the present work material from the following localities (Figure VII.2) has been studied.

### (i) *The Kangerdlugssuaq Intrusion*

This exceptionally large syenite pluton is roughly circular with a diameter of more than 30 km. It contains both oversaturated and undersaturated rocks and was emplaced centrally in the Kangerdlugssuaq domal structure. Several workers have dated the area using various methods. BECKINSALE et al., using the K-Ar method,<sup>46</sup> and PANKHURST et al.,<sup>105</sup> using the Rb/Sr method, obtain a mean age of  $49.2 \pm 0.6$  m.y. BECKINSALE et al.<sup>46</sup> have also dated amphibole from the Kap Boswell syenite, which is in good agreement with results for Kangerdlugssuaq. Fission track dating of zircons from Skaergaard, made by BROOKS and GLEADOW,<sup>43</sup> yields an age of  $54.6 \pm 1.7$  m.y, showing the emplacement to be close to 50 m.y. However, our FT ages (Table VII.2) and the ages reported more recently by GLEADOW and BROOKS<sup>48</sup> are in close agreement, and we also conclude that there must have been a slow cooling at former deep levels, which now lie at the surface due to erosion of as much as 6 km of the overlying dome. The apatite cooling age (which records cooling through the approximate 100°C isotherm (see section V) is somewhat in agreement with that reported earlier.<sup>26</sup>

Our new fission track ages for zircon from the Kangerdlugssuaq intrusion (Table VII.2) have a weighted mean of  $49.6 \pm 2.9$  m.y. These figures are in good agreement with the ages reported previously.<sup>43</sup> The apatite ages from the above intrusion give a mean age of  $38.2 \pm 2.2$  m.y, significantly lower than the ages obtained for zircons, suggesting prolonged cooling in this area followed later by uplift and erosion. It is suggested,<sup>45</sup> for the area south of Scoresbysund centred on the fjord of Kangerdlugssuaq, that an analysis of the physiographic elements of landscape indicates the major uplift to have occurred in two phases. A project using both K/Ar and fission track dating is presently underway in order to clarify this. Further studies show that on approaching the Kangerdlugssuaq district the pre-syenitic basalt become increasingly tilted upwards and are finally completely dissected to expose a core of Precambrian gneisses centred on Kangerdlugssuaq. These gneisses form jagged alpine peaks rising to around 2.5 km and it is clear that erosion has been active for a much longer time than in outlying basaltic areas. By making certain simple and reasonable assumptions it is

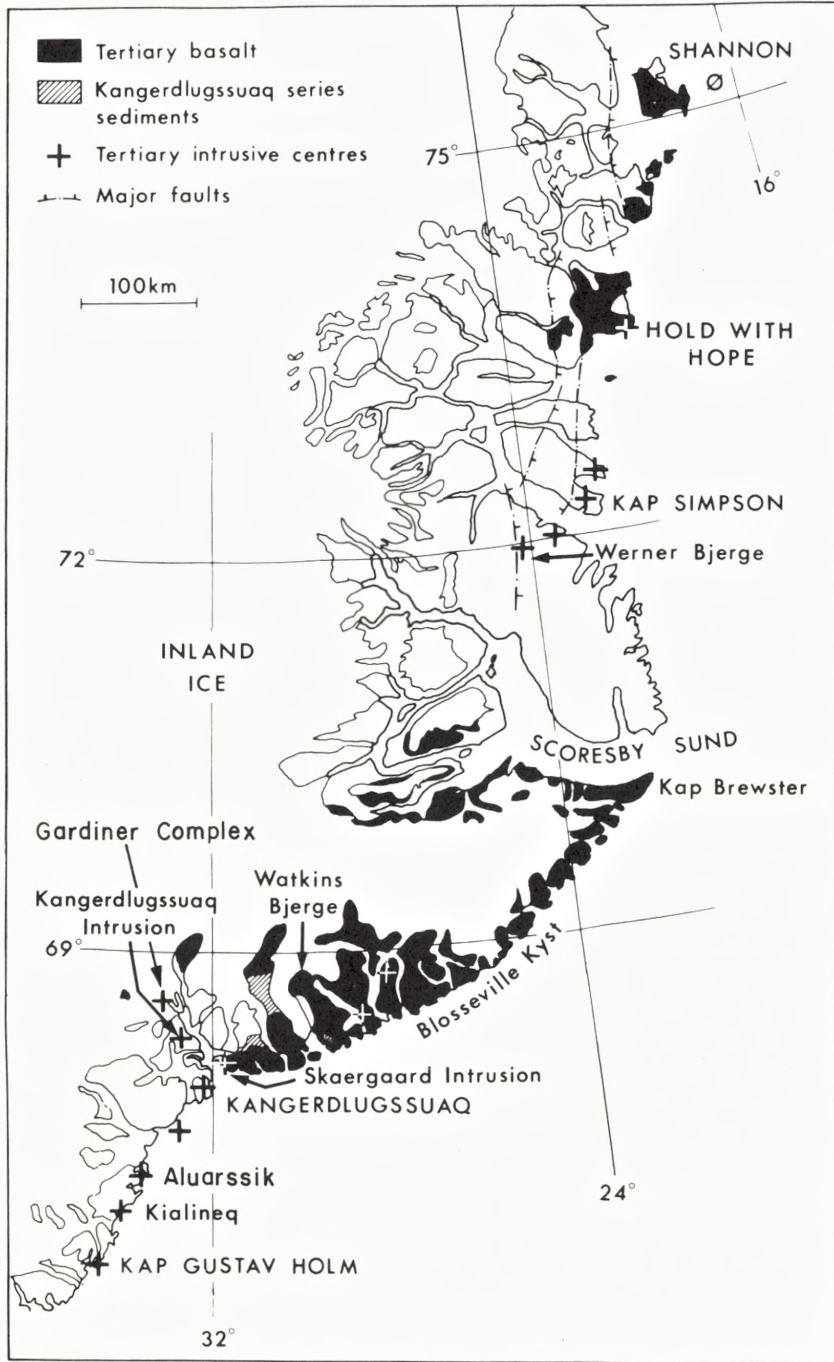


Fig. VII.2. Geological map of East Greenland.

*Table VII.2*  
*Fission track results for minerals from Greenland*

Sample location	Lab. symbols	$Q_s$ ( $\text{cm}^{-2}$ )	$Q_i$ ( $\text{cm}^{-2}$ )	$\Phi$ (nvt)	R	N	F.T. age (m.y.)
1. Apatite. Gardiner, East Greenland.	ZR10	$3.90 \times 10^4$	$1.8 \times 10^5$	$3.8 \times 10^{15}$	0.948	9	$50.7 \pm 2.8$
	ZR02	$8.40 \times 10^4$	$3.9 \times 10^5$	—	0.858	9	$50.4 \pm 3.1$
	ZR03	$7.32 \times 10^4$	$3.3 \times 10^5$	—	0.991	11	$51.9 \pm 3.2$
	ZR09	$6.72 \times 10^4$	$3.2 \times 10^5$	—	0.981	10	$48.8 \pm 2.9$
2. Apatite. Aliurssik, East Greenland.	AA101	$1.75 \times 10^5$	$2.73 \times 10^6$	$8.83 \times 10^{15}$	0.953	7	$34.9 \pm 1.8$
	AA102	$2.45 \times 10^5$	$4.12 \times 10^6$	—	0.967	6	$32.4 \pm 1.7$
	AA104	$1.64 \times 10^5$	$2.57 \times 10^6$	—	0.880	6	$34.7 \pm 2.0$
	AA105	$1.42 \times 10^5$	$2.12 \times 10^6$	—	0.995	9	$36.5 \pm 1.6$
	AA106	$1.52 \times 10^5$	$2.31 \times 10^6$	—	0.987	8	$35.8 \pm 1.9$
3. Apatite Kangerdlugssuaq, East Greenland.	KT15	$4.7 \times 10^4$	$2.8 \times 10^5$	$3.84 \times 10^{15}$	0.754	5	$38.8 \pm 2.3$
	KT16	$4.3 \times 10^4$	$2.8 \times 10^5$	—	0.895	6	$36.3 \pm 2.0$
	KT17	$4.2 \times 10^4$	$2.4 \times 10^5$	—	0.982	5	$41.4 \pm 2.1$
	KT18	$3.9 \times 10^4$	$2.5 \times 10^5$	—	0.923	7	$36.9 \pm 2.4$
	KT19	$8.4 \times 10^4$	$5.0 \times 10^5$	—	0.897	6	$39.7 \pm 2.3$
	KT19A	$5.4 \times 10^4$	$3.4 \times 10^5$	—	0.985	8	$37.6 \pm 2.1$
	KT20	$5.6 \times 10^4$	$3.5 \times 10^5$	—	0.727	5	$37.9 \pm 2.6$
	KT22	$4.8 \times 10^4$	$3.1 \times 10^5$	—	0.895	7	$36.6 \pm 2.0$
4. Sphenes. Gardiner, East Greenland.	BK1	$5.3 \times 10^5$	$1.70 \times 10^6$	$2.69 \times 10^{15}$	0.895	6	$51.6 \pm 2.6$
	BK2	$4.5 \times 10^5$	$1.50 \times 10^6$	—	0.974	8	$49.7 \pm 2.2$
	BK3	$4.9 \times 10^5$	$1.62 \times 10^6$	—	0.747	6	$50.1 \pm 2.4$
	BK4	$6.1 \times 10^5$	$2.10 \times 10^6$	—	0.985	5	$48.1 \pm 1.9$
	BK5	$5.31 \times 10^5$	$1.79 \times 10^6$	—	0.991	7	$47.5 \pm 2.1$
	BK7	$5.62 \times 10^5$	$1.64 \times 10^6$	—	0.985	8	$55.3 \pm 1.9$
	BK8	$7.25 \times 10^5$	$2.38 \times 10^6$	—	0.874	7	$50.5 \pm 2.4$
	BK9	$6.41 \times 10^5$	$2.14 \times 10^6$	—	0.768	13	$49.6 \pm 2.6$
	BK10	$4.25 \times 10^5$	$1.33 \times 10^6$	—	0.845	8	$52.9 \pm 2.8$
	5. Zircon. Gardiner, East Greenland.	AG21	$5.23 \times 10^5$	$1.45 \times 10^6$	$2.40 \times 10^{15}$	0.994	7
AG28		$4.84 \times 10^5$	$1.32 \times 10^6$	—	0.932	5	$54.2 \pm 2.1$
AG29		$4.75 \times 10^5$	$1.30 \times 10^6$	—	0.897	5	$53.9 \pm 2.3$
AG32		$5.41 \times 10^5$	$1.53 \times 10^6$	—	0.983	6	$52.2 \pm 1.8$
AG39		$6.22 \times 10^5$	$1.75 \times 10^6$	—	0.763	8	$52.5 \pm 2.4$
6. Zircon. Aliuarssik, East Greenland.	AZ91	$3.24 \times 10^5$	$2.12 \times 10^6$	$3.84 \times 10^{15}$	0.973	6	$36.2 \pm 1.1$
	AZ95	$3.51 \times 10^5$	$2.24 \times 10^6$	—	0.895	7	$37.1 \pm 1.2$
	AZ98	$2.84 \times 10^5$	$1.92 \times 10^6$	—	0.932	6	$35.0 \pm 1.1$
	AZ99	$3.12 \times 10^5$	$2.11 \times 10^6$	—	0.981	8	$35.0 \pm 1.0$
	AZ103	$4.03 \times 10^5$	$2.70 \times 10^6$	—	0.871	6	$35.4 \pm 1.2$

7. Zircon.	KZ49	$9.34 \times 10^5$	$2.75 \times 10^6$	$2.39 \times 10^{15}$	0.892	6	$49.9 \pm 3.0$
Kangerdlugssuaq,	KZ53	$8.62 \times 10^5$	$2.63 \times 10^6$	—	0.954	6	$48.2 \pm 2.8$
East Greenland.	KZ57	$8.50 \times 10^5$	$2.45 \times 10^6$	—	0.983	8	$51.5 \pm 3.1$
	KZ59	$4.73 \times 10^5$	$1.52 \times 10^6$	—	0.980	11	$45.8 \pm 3.0$
	KZ60	$4.70 \times 10^5$	$1.34 \times 10^6$	—	0.894	8	$51.6 \pm 3.1$
	KZ65	$8.32 \times 10^5$	$2.40 \times 10^6$	—	0.943	7	$50.5 \pm 2.9$
8. Phlogopite.	PL107	$5.15 \times 10^5$	$3.31 \times 10^6$	$5.28 \times 10^{15}$	0.975	8	$50.6 \pm 2.1$
Gardiner,	PL109	$5.45 \times 10^5$	$3.43 \times 10^6$	—	0.891	7	$51.4 \pm 2.0$
East Greenland.	PL110	$3.72 \times 10^5$	$2.25 \times 10^6$	—	0.774	5	$53.7 \pm 2.5$
	PL111	$4.66 \times 10^5$	$3.03 \times 10^6$	—	0.981	7	$50.0 \pm 2.0$
	PL112	$4.35 \times 10^5$	$2.85 \times 10^6$	—	0.672	9	$49.8 \pm 2.3$
	PL113	$5.04 \times 10^5$	$3.11 \times 10^6$	—	0.743	5	$52.7 \pm 2.2$

$q_s$  is the spontaneous track density,  $q_i$  the induced track density,  $n$  the thermal neutron dose (nvt),  $N$  the number of grains counted, and  $R$  the correlation coefficient.

possible to construct an original land surface which shows that the area was domed up over some 300 km and to a height of around 6.5 km above the present sea level, or 4 km relative to the surrounding terrain. The Watkins Bjerge, which reaches a height of nearly 4 km, is part of the eroded remnants of this dome. In accordance with the ideas of GASS,<sup>106</sup> this suggests that the dome developed in association with the intrusion of the Kangerdlugssuaq syenites about 50 m.y ago. Our fission track ages (Table VII.2) show distinct cooling in this area.

#### (ii) The Gardiner Intrusion

According to NIELSEN and BROOKS<sup>107</sup> and FRISCH and KEUSEN,<sup>108</sup> this intrusion is a ring complex composed of ultramafic and melilitite bearing rocks of a rather unusual type situated at the head of the Kangerdlugssuaq Fjord on the continental side of the province where the plateau basalts are strongly thinned. It is believed to be derived from a nephelinitic parent magma and its age is similar to that of the Kangerdlugssuaq intrusion. The concordance of apatite, sphene, phlogopite and zircon fission track ages (Table VII.2) as well as agreement with K/Ar ages<sup>45</sup> for mica indicates that it was emplaced at shallow levels and cooled rapidly. This conclusion is also in accord with field evidence. Small variations in the fission track ages depend on the rates of annealing of spontaneous tracks in the minerals; each mineral anneals over its own specific temperature range. The annealing behaviour of zircon, sphene and apatite has been described previously.<sup>21, 23, 94</sup> The mineral phlogopite was also selected for study, especially with respect to track retention and annealing characteristics; hence the detailed experiments described in section V on the "ranges" of both spontaneous and induced fission fragments. Phlogopite records cooling through a 195°C isotherm which is somewhat higher than reported earlier for apatite. The closing temperature for this mineral is lower than that for muscovite.

The zircon FT ages (Table VII.2) agree closely with previous K/Ar results for this complex. The suggestion is that there was a virtually simultaneous intrusion of different bodies, followed by rapid cooling to a temperature below 195°C. Samples of sphene, phlogopite and apatite yielded FT ages between  $47 \pm 2$  and  $54 \pm 2$  m.y. There is therefore no evidence in the present work for ages older than about 55 m.y indicating that up to that time at least the region was so thermally unstable that even tracks in zircon were completely annealed. However, the Gardiner complex is believed to be of a similar emplacement age to that of the Kangerdlugssuaq intrusion, confirming that rapid cooling took place in the area. All of this, and the petrological and field evidence,<sup>108</sup> suggests the Gardiner intrusion to be a very high level one indeed.

(iii) *Aliuarssik*

This island in the Kialineq district is partially occupied by a circular granitic intrusion. Several studies indicate that magmatic activity in this area was substantially later than that in the Kangerdlugssuaq area, and possibly occurred in response to major readjustments of plate motions which are known to have taken place at this time. The apatite and zircon results reported here (Table VII.2) confirm the dating of this activity and also that cooling again took place rapidly. This is in agreement both with the previous results and with the field evidence, since the granite is strongly miarolitic, a texture characteristic of shallow level or sub-volcanic intrusions. BECKINSALE et al.<sup>46</sup> give K/Ar dates for biotite and amphibole of  $37.5 \pm 1.6$  and  $49.0 \pm 3.1$  m.y respectively, whilst a Rb/Sr age of  $35 \pm 2$  m.y for various rocks has been reported by BROWN et al.<sup>47</sup> The same authors have made K/Ar measurements on the minerals biotite and hornblende yielding figures of 35.9 m.y and 35.4 m.y respectively. The fission track age we report ( $35 \pm 1.1$  m.y) once more indicates a rather rapid cooling at about this time, in support of earlier work by GLEADOW and BROOKS,<sup>48</sup> who find for this granite a weighted mean of zircon and apatite FT ages of  $36.8 \pm 0.9$  m.y. They also find similar ages for the Qajarsak granite and Bjørn syenite using zircon samples. The measured ages confirm that the last thermal event at about 35 m.y did not affect the fossil tracks stored in zircon and sphene, as they show no significant shrinkage. However, the event has had an effect on the measured ages of apatites.



## VIII. Conclusion

It is a basic assumption of fission track dating methods that the ratio of track to bulk chemical etch rate is unity, which is to say that the revelation of both spontaneous and induced tracks is the same under identical etching and counting conditions. In addition as the experiments with chabazite and other minerals clearly show, because of a fundamental anisotropic etching behaviour it is necessary that only surfaces with identical etching characteristics be used for dating purposes. For zeolites both population<sup>†</sup> (internal) and external<sup>††</sup> detection procedures can be followed providing that certain intrinsic limitations are appreciated. For example, due to varying registration geometry, surface etching efficiency and angular track anisotropy, the use of external detectors should be avoided if the sample consists of tiny mineral grains mounted in epoxy resin. Violation of the assumption of identical registration and etching conditions makes the final fission track ages quite unreliable.

Annealing experiments show that the thermal stability of tracks in chabazite is lower than in sphene, garnet, epidote, allanite and hornblende. Data from these and corresponding experiments on track shrinkage suggest that ages determined by applying the fission track method to zeolites will be slightly affected by annealing. Nevertheless the basic FT method is considered to be generally applicable to the dating of zeolites.

Similar annealing experiments on phlogopite indicate that fission fragment tracks are unstable, and confirm that the degree of instability varies from mineral to mineral. Fossil tracks can be erased in minerals during intense metamorphic episodes, thus resetting the geological clock. For the case of phlogopite in particular, extrapolation of the experimentally determined temperatures for annealing suggests that a temperature of 195°C will erase all tracks in 10<sup>6</sup> years.

The fission track ages obtained for samples from the Faeroe Islands lead us to the conclusion that onshore volcanism was limited to a span of time between  $41.6 \pm 1.1 \times 10^6$  and  $55.4 \pm 2.6 \times 10^6$  years ago. It is likely that this volcanic activity coincided, at least in part, with either global or more regional movements of both a plate-tectonic and epeirogenic character in East Greenland. Volcanism and epeirogenesis are supposed to reflect major processes taking place in the upper mantle and are, therefore, intimately associated with plate tectonic events.

The observed distribution of ages in the Faeroe Islands is probably regional, with the youngest ages in the north-eastern part of the islands reflecting more prolonged cooling in that area. Ages from the Lower Series on Suduroy and Mykines, which are close to the currently accepted age for volcanism, indicate that in the south and west of the

† The average spontaneous track density is here measured in one sample, and the induced track density in a separate sample which is annealed prior to irradiation.

†† Spontaneous tracks are etched in the mineral grains and induced tracks in an adjacent track detector of either muscovite or lexan polycarbonate.

islands the lavas underwent rapid cooling either as a result of lack of burial by significant amounts of overlying material, or as a result of rapid uplift. Such a rapid uplift is most likely due to dome-shaped structures believed to be present offshore to the north-west of Mykines, and under Suduroy. These domes, although occurring on much smaller scale, invite comparison with East Greenland, where a large uplift was raised after the basaltic volcanism, and rapidly dissected by erosion. For the Kangerdlugssuaq area in particular it is proposed that there is clear evidence for strong doming and regional uplift about 50 m.y ago, giving rise to the Kangerdlugssuaq intrusion at a high level in the crust, close to the unconformity between Precambrian gneisses and the overlying tertiary basalts. With respect to identification of the 40–55 m.y event as that occurring during continental breakup it should be noted that this is by far the most widespread and voluminous event in the North Atlantic. There is separate evidence for a volume of basalts in East Greenland of the order of  $2 \times 10^5 \text{ km}^3$ , and a similar volume of magma in dikes. In addition, considerable volumes of basalts, believed to be contemporaneous, are found in the Faeroe Islands.

The north Atlantic area is of particular interest, not only because of its position between the Eurasian and American land masses, but also with respect to faunal and floral migration.

#### *Acknowledgements*

The authors are grateful to Mr. Ole Jørgensen for donation of the zeolite samples, to Dr. R. L. Fleischer for supplying the glass dosimeters, and to Dr. R. McCorkell for plastic detectors. The support of the Danish Natural Science Research Council and the DANIDA office of the Danish Foreign Ministry is gratefully acknowledged.